10.1071/EN17158_AC

Environmental Chemistry 2017, 14(8), 515-524

Supplementary Material

Deconstructing the redox cascade:
What role do microbial exudates (flavins) play?

Ekaterina Markelova,[A,B,*] *Christopher T. Parsons,*[A] *Raoul-Marie Couture,*[A,C] *Christina M. Smeaton,*[A] *Benoit Madé ,*[D] *Laurent Charlet,*[A,B] *Philippe Van Cappellen*[A]

[A]Ecohydrology Research Group, Department of Earth and Environmental Sciences and Water Institute, University of Waterloo, 200 University Ave. W, Waterloo, ON N2L 3G1, Canada.
[B]Institut des Sciences de la Terre (ISTerre), Université Grenoble Alpes, P.O. Box 53, F 38041 Grenoble, France.
[C]Norwegian Institute for Water Research-NIVA, Gaustadalléen 21, 0349 Oslo, Norway.
[D]Andra, National Radioactive Waste Management Agency, R&D Division, Transfer Migration Group, 1/7 rue Jean Monnet, 92298 Chatenay Malabry Cedex, France.
[*]Corresponding author. Email: emarkelo@uwaterloo.ca

Goethite synthesis

Goethite was synthesized following Varanda et al. (2002) and Cornell & Schwertmann (2003).[1,2] Briefly, a ferric iron salt ($Fe(NO_3)_3 \cdot 9H_2O$, EMD Chemicals) was dissolved in Milli-Q water. The pH was then raised from 3 to 10 with KOH to precipitate ferrihydrite. The suspension was heated for 2 days at 40 °C and then for 3 days at 60 °C before being poured into dialysis bags (7 Spectra/Por Dialysis Membrane MWCO:1000). Dialysis was performed in a Milli-Q water bath (10 L), replaced every day for 7 days until bath conductivity decreased from 2118 to 0.88 µS cm^{-1}. The purified precipitate was freeze-dried, ground, and identified as goethite by XRD (PANalytical Empyrean II with Cu-α cathode tube).

Ammonium assimilation into growing biomass

The missing NH_4^+ in Exp. III can be explained by NH_4^+ assimilation into growing biomass.[3] Microbial ATP concentrations reached much higher levels in Exp. III compared to Exp. IV. During the first N_2 sparging period of Exp. III, microbial ATP rose from 23 to 138 nM. In contrast, the maximum microbial ATP concentration at the end of Exp. IV was only 5.2 nM. Based on the changes in microbial ATP, we estimate that biomass growth in Exp. III was at least 20 times higher than in Exp. IV. Microbial ATP concentrations calibrated against known *S. oneidensis* cell numbers ($4.6 \pm 0.6 \times 10^{-10}$ nM $cell^{-1}$, see calibration curve in Fig. S1) imply that the biomass should have reached 2×10^{11} cells L^{-1} by the end of the first N_2 sparging period of Exp. III. Using the nitrogen content of *Escherichia coli* (24 fg N $cell^{-1}$),[4] the corresponding nitrogen assimilation by the newly formed biomass would have been around 0.4 mM, which would account for a large fraction of the missing NH_4^+ in Exp. III.

Table S1. Composition of the artificial groundwater (AGW) used in Experiments II, III, IV and V.

Chemical	mmol L^{-1}
KH_2PO_4	0.05
$MgSO_4$, $7H_2O$	0.6
$MgCl_2$	0.4
NH_4Cl	0.1
KOH	8.0
KNO_3	1.0
Na-$C_3H_5O_3$	18.0
MOPS ($C_7H_{15}NO_4S$)	20.0

Table S2. Standard redox potentials at pH 7 and 25 °C for common microbial redox couples that help maintain the intracellular redox balance.

Microbial redox couples	$E_H°'$ (mV), pH 7	Reference
NAD^+/NADH	-316	[5]
$NADP^+$/NADPH	-315	[5]
Cytochrome c_3 ox/red	-290	[6]
TrxSS/$Trx(SH)_2$	-248	[5]
GSSG/2GSH	-240	[7]
Cys/CySS	-230	[5]
FAD/$FADH_2$	-220	[6]
FMN/$FADH_2$	-220	[6]

Table S3. Half reduction reactions of terminal electron acceptors used in the experiments, with corresponding equilibrium constants (log K) and standard state redox potentials (E^0) relative to the standard hydrogen electrode at pH 0 and pH 7.5.

Half-reaction	log K	E^0, mV (pH=0)[a]	E^0, mV (pH=7.5)[b]
Oxygen reduction			
$O_2 + 4H^+ + 4e^- \rightarrow 2H_2O$	83.2	1230	779
$O_2 + 2H^+ + 2e^- \rightarrow H_2O_2$	23.2	686	242
Nitrate reduction			
$NO_3^- + 2H^+ + 2e^- \rightarrow NO_2^- + H_2O$	28.4	845	394
$NO_3^- + 10H^+ + 8e^- \rightarrow NH_4^+ + 3H_2O$	119.2	881	317
Nitrite reduction			
$NO_2^- + 8H^+ + 6e^- \rightarrow NH_4^+ + 2H_2O$	90.6	892	290
Goethite reduction			
α-$FeOOH_{(s)} + 3H^+ + 1e^- \rightarrow Fe^{2+} + 2H_2O$	11.31	769	-561

[a] Based on Essington (2004)[8] for standard conditions at 25 °C.

[b] Values calculated using PHREEQC (phreeqc.dat) implying {red}={ox}= 1 mol L^{-1} and solution equilibrium with goethite (SI = 0).

Table S4. Chemical concentrations, E_H, and pH measured at the end of the redox subzones identified in Fig. 2. Dissolved O_2 concentrations were estimated assuming equilibrium with atmospheric air (A – C) and with N_2 gas (D – H).

	pH	E_H mV	O_2 mol l^{-1}	NO_3^- µmol l^{-1}	NO_2^- µmol l^{-1}	NH_4^+ µmol l^{-1}	$Fe^{2+}_{(aq)}$ µmol l^{-1}
A_1	7.45	502	2.7×10^{-4}	–	–	–	–
A_2	7.49	501	2.7×10^{-4}	–	–	–	–
B_1	7.41	360	2.7×10^{-4}	991	<DL	89	–
B_2	7.42	372	2.7×10^{-4}	929	<DL	80	–
C_1	7.82	287	2.7×10^{-4}	<DL	<DL	<DL	–
C_2	8.04	310	2.7×10^{-4}	<DL	<DL	<DL	–
C_3	7.28	277	2.7×10^{-4}	818	31	250	<DL
C_4	7.31	282	2.7×10^{-4}	481	285	260	<DL
D_1	7.63	108	1×10^{-16}	–	–	–	–
D_2	7.64	118	1×10^{-16}	–	–	–	–
E_1	7.41	55	1×10^{-16}	991	<DL	89	–
E_2	7.41	45	1×10^{-16}	932	<DL	68	–
E_3	7.28	64	1×10^{-16}	922	23	192	<DL
E_4	7.29	42	1×10^{-16}	765	75	201	<DL
F_1	7.55	-10	1×10^{-16}	556	118	144	–
F_2	7.44	-5	1×10^{-16}	<DL	30	866	<DL
G_1	8.02	-230	1×10^{-16}	<DL	<DL	<DL	–
G_2	7.49	-279	1×10^{-16}	<DL	<DL	155	7.5
H	7.55	-315	1×10^{-16}	<DL	<DL	157	46

Table S5. Summary of practical recommendations for the use of Pt electrodes.

Recommendation	Action	Ref
Correction for temperature with respect to the standard hydrogen electrode (SHE)	For example, at 20 °C the correction value of 211 mV should be added to the E_H value measured by the Pt electrode with an Ag|AgCl – 3 M KCl reference electrode. The correction value is calculated as the difference in the potentials of SHE (439 mV, tabulated) and the reference electrode (228 mV, tabulated) at a specific temperature.	[9]
Test for electrode accuracy against a standard solution	For example, at 20 °C the E_H value of ZoBell's standard solution measured by the Pt electrode (Ag|AgCl – 3 M KCl) is 250 mV. The correction of the measured value for SHE results in E_H(SHE) = 461 mV (250 mV + 211 mV), which is 18 mV higher than the tabulated E_H(SHE) of ZoBell's solution (443 mV). The difference between theoretical and practical potentials of ZoBell's solution is commonly accepted up to ±30 mV. The correction of measured E_H by addition/subtraction of observed difference (e.g, -18 mV in this example) is recommended.	[10]
Monitoring of pH and E_H in situ	Measured E_H should be recorded along with pH under the same conditions. Further correction of E_H readings to the pH of interest should account for the actual ratio of H^+ to e^-, which is not necessarily equal to 1 (59 mV). Interference of the E_H signal due to close proximity of the pH and E_H reference electrodes can be overcome by using a common reference electrode for both measurements.	[11][12]
Electrode cleaning	A soft material (e.g., glass fibre, lapping pads) can be used to polish the Pt surface to erase the electrode "history" of Pt-oxides and prevent the drift of electrochemical potential.	[13][14]
Stabilization of sample flow velocity	In batch suspensions flow velocity can be controlled by adjusting the stirring speed, which should be recorded along with E_H data. In systems where flow velocity may not be easily controlled (e.g., measurements within rivers), the electrode surface should be shielded from changes to flow.	[15]
Addition of an inert electrolyte to water samples with low ionic strength less than 0.005 M	The addition of 9 mM NaCl to water sample improves electrode performance likely due to a combination of the decreased internal resistance and increased exchange current facilitated by the presence of chloride ions adsorbed at the Pt surface.	[16][17]

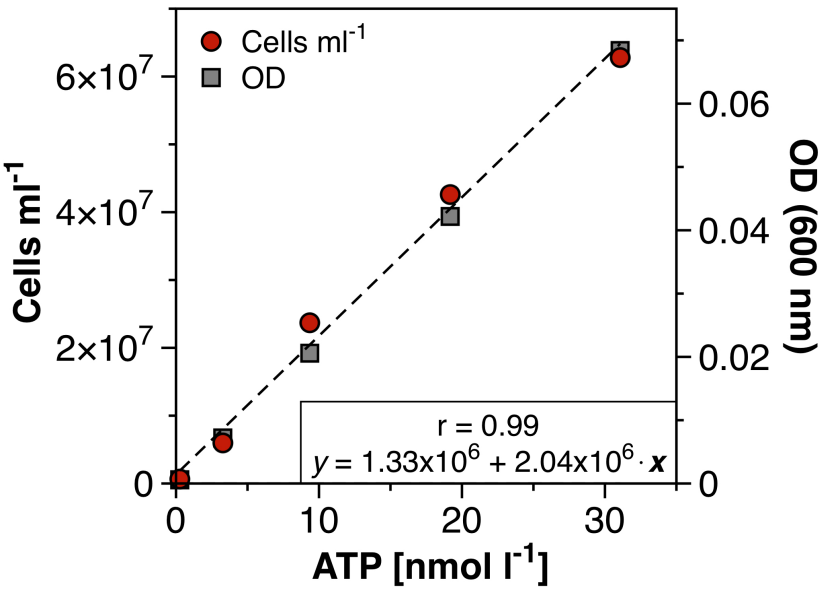

Fig. S1. Calibration curve of ATP concentrations (x) as a function of the cell density per 1 ml of bacterial suspension (y) plotted against optical density (OD_{600}). Average concentration of ATP in a cell of *Shewanella oneidensis* MR-1 is $4.6\times10^{-10} \pm 6.2\times10^{-11}$ nM cell^{-1}.

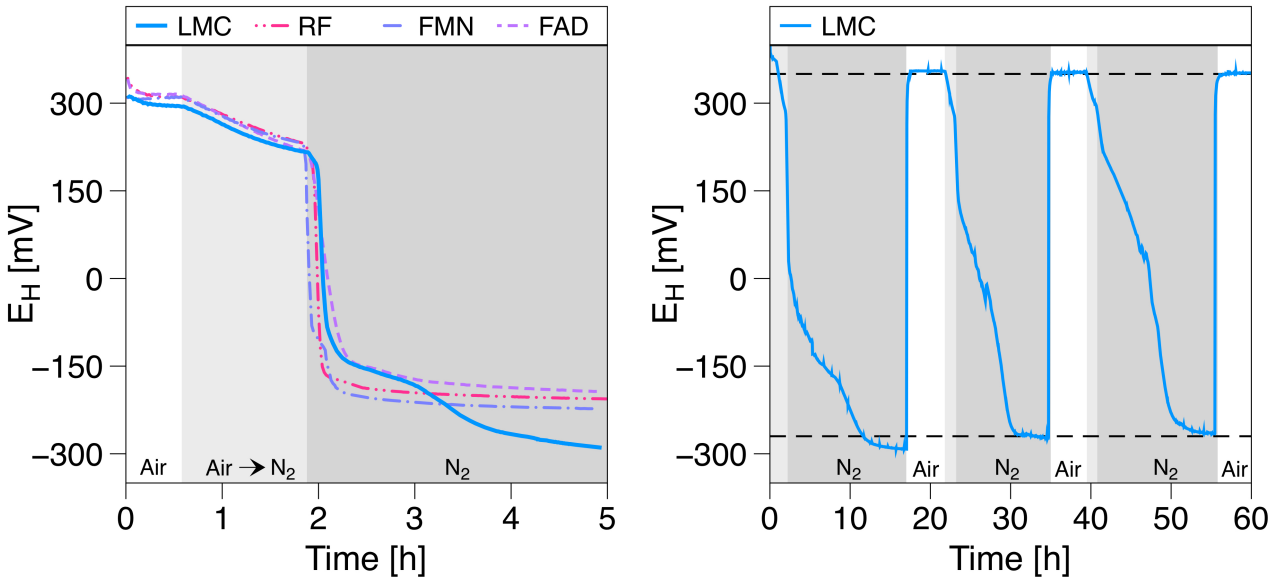

Fig. S2. Examples of time-series E_H data recorded at 30 °C in solutions containing 20 µM lumichrome (LMC), riboflavin (RF), flavin mononucleotide (FMN), and flavin adenine dinucleotide (FAD) (left figure) and 0.5 µM LMC (right figure) dissolved in artificial groundwater. During the initial phase (no shading) the solutions are purged with air. The intermediate phase (light shading) corresponds to the period of N_2 sparging during which the dissolved O_2 concentration decreased, and the final phase (darker shading) to the period of N_2 sparging when dissolved O_2 was undetectable. The right figure shows the results obtained during successive periods of N_2 and air sparging.

Table S6. Redox potentials of oxidized and photoreduced flavins dissolved in artificial groundwater at temperature 30 ºC.

Flavins	Concentration 5×10^{-7} M		Concentration 2×10^{-5} M	
	Oxidized	*Reduced*	*Oxidized*	*Reduced*
Lumichrome (LMC)	+355 mV	-295 mV	+295 mV	-290 mV
Riboflavin (RF)	+350 mV	-200 mV	+270 mV	-225 mV
Flavin mononucleotide (FMN)	+343 mV	-225 mV	+310 mV	-222 mV
Flavin adenine dinucleotide (FAD)	+350 mV	-194 mV	+315 mV	-180 mV

References

[1] L.C. Varanda, M.P. Morales, J.M. Jafelicci, C.J. Serna, Monodispersed spindle-type goethite nanoparticles from FeIII solutions. *J. Mater. Chem.* **2002**,*12*,3649–3653.

[2] R.M. Cornell, U. Schwertmann, *The Iron Oxides: Structure, Properties, Reactions, Occurences and Uses.* **2003** (Wiley_VCH Verlag GmbH & Co. KGaA, Weinheim)

[3] C. Cruz-García, A.E. Murray, J. a Klappenbach, V. Stewart, J.M. Tiedje, Respiratory nitrate ammonification by Shewanella oneidensis MR-1. *J. Bacteriol.* **2007**,*189*,656–662.

[4] K. Fagerbakke, M. Heldal, S. Norland, Content of carbon, nitrogen, oxygen, sulfur and phosphorus in native aquatic and cultured bacteria. *Aquat. Microb. Ecol.* **1996**,*10*,15–27.

[5] A. Kumar, A. Farhana, L. Guidry, V. Saini, M. Hondalus, A.J.C. Steyn, Redox homeostasis in mycobacteria: the key to tuberculosis control? *Expert Rev. Mol. Med.* **2011**,*13*,e39.

[6] K.O. Konhauser, *Introduction to Geomicrobiology*. **2007** (Blackwell Science)

[7] I. Kranner, S. Birtić, K.M. Anderson, H.W. Pritchard, Glutathione half-cell reduction potential: A universal stress marker and modulator of programmed cell death? *Free Radic. Biol. Med.* **2006**,*40*,2155–2165.

[8] M.E. Essington, *Soil and Water Chemistry: An Integrative Approach*. **2004** (CRC Press LLC)

[9] C.A.J. Appelo, D. Postma, *Geochemistry, Groundwater and Pollution*. **2005** (CRC Press LLC)

[10] J. Schuring, H.D. Schulz, W.R. Fischer, *Redox: Fundamentals, Processes and Applications*. **1999** (Springer)

[11] L.G.M.B. Becking, I.R. Kaplan, D. Moore, Limits of the Natural Environment in Terms of pH and Oxidation-Reduction Potentials. *J. Geol.* **1960**,*68*,243–284.

[12] L.F. Hewitt, *Oxidation-reduction potentials in bacteriology and biochemistry*. **1950** (Baltimore, Williams and Wilkins)

[13] D.K. Nordstrom, E.A. Jenne, J.. Ball, in: *Chemical Modeling in Aqueous Systems: Speciation, Sorption, Solubility and Kinetics* (Ed E.A. Jenne) **1979**, pp. 51–80 (Am. Chem. Soc. Symp. Ser. No 93, Washington, DC).

[14] L. Aldous, R.G. Compton, The mechanism of hydrazine electro-oxidation revealed by platinum microelectrodes: role of residual oxides. *Phys. Chem. Chem. Phys.* **2011**,*13*,5279.

[15] E.E. Garske, M.R. Schock, An Inexpensive Flow-Through Cell and Measurement System for Monitoring Selected Chemical Parameters in Ground Water. *Ground Water Monit. Remediat.* **1986**,*6*,79–84.

[16] T.J. Grundl, D.L. Macalady, Electrode measurement of redox potential in anaerobic ferric/ferrous chloride systems. *J. Contam. Hydrol.* **1989**,*5*,97–117.

[17] S. Peiffer, O. Klemm, K. Pecher, R. Hollerung, Redox measurements in aqueous solutions — A theoretical approach to data interpretation, based on electrode kinetics. *J. Contam. Hydrol.* **1992**,*10*,1–18.